MVA2007 IAPR Conference on Machine Vision Applications, May 16-18, 2007, Tokyo, JAPAN

A New Method for Auroral Oval Detection in FUV Imagery

Chunguang Cao Timothy S. Newman
Department of Computer Science
University of Alabama in Huntsville
Huntsville, AL 35899
E-mail: {ccao, tnewman}@cs.uah.edu

Glynn A. Germany
Center for Space Plasma
and Aeronomic Research
Univ. of Alabama in Huntsville
Huntsville, AL 35899

Jim F. Spann
National Space Science
and Technology Center
Huntsville, AL 35805

Abstract

A new fully automatic method for detecting auroral ovals in images produced by the NASA IMAGE satellite's Far Ultra Violet (FUV) sensor is introduced. The method exploits the shape characteristics of the auroral oval and utilizes domain knowledge. The shape exploitation involves an efficient Hough-based process. Experimental results show that the new method can accurately detect the auroral oval in the FUV images.

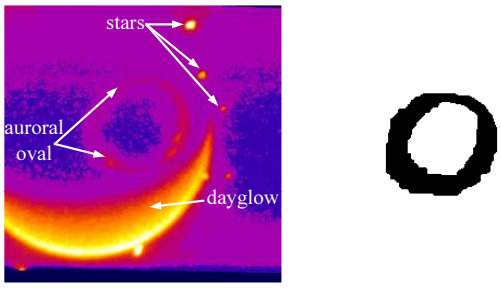

(a) 20003460020 (b)

Figure 1. (a) A sample FUV image, (b) Manual auroral oval detection result

1. Introduction

At the speed of several hundred or more kilometers per second, solar wind constantly strikes the Earth's magnetic field. The interaction between the solar wind and the magnetic field causes the spectacular phenomena of the aurorae. Study of auroral activity is important due to its helpfulness in analyzing high-latitude ionosphere-thermosphere-magnetosphere (ITM) behaviors. One source of a large collection of imagery for study of auroral activity is the Far Ultra Violet (FUV) sensor on board the NASA Imager for Magnetopause-to-Aurora Global Exploration (IMAGE) satellite. Since the start of its mission in March 2000, FUV has so far produced over 1.5 million images.

Many auroral physics studies require determination of the location of auroral activity in imagery. The auroral activity occurs within a ring, called the auroral oval. Manual determination of the auroral oval in an image is somewhat tedious, and, sometimes, difficult. Fig. 1(a) shows a sample FUV image. Fig. 1(a) (and the others of FUV images) in this paper are identified by the date and time of capture (e.g., Fig. 1(a) was captured at 00:20 on the 346th day of year 2000). Fig. 1(a) also has labels for some features of interest overlaid on it. This figure, and the other FUV images shown in this paper, are contrast-enhanced using histogram equalization for viewing clarity. Fig. 1(b) shows a manual auroral oval detection result for this image. From Fig. 1(a), it can be seen that the intensity contrast around the auroral oval remains very low even after enhancement; low contrast is a challenge for automated detection. Yet automated methods to detect the auroral oval in imagery can be beneficial, especially since study of auroral behavior over time requires consideration of a series of images. Besides the low level of contrast, another major complication for both manual and automatic detection methods is the dayglow contamination in many FUV images. Dayglow is caused by emission of the excited atoms and molecules in the upper atmosphere [7]. The bright crescent-shaped part near the bottom of Fig. 1(a) is an example of dayglow. In FUV, dayglow intensities usually are significantly higher (e.g., as much as an order of magnitude or more) than auroral intensities. In addition, the presence of bright stars, which are also present in Fig. 1(a), can complicate processing, especially for automated methods.

In this paper, a method for automatic and accurate auroral oval detection in FUV imagery is introduced. The method is, to our knowledge, the first automatic method for auroral oval detection in FUV images. The new method is motivated by the method of Cao et al. [1] for Polar Ultraviolet Imager (UVI) images. Although several methods, including the Cao et al. method, have been successfully ap-

(a) (b) (c) (d)

Figure 2. (a) PCNN-based method result, (b) HKM result, (c) AMET result, (d) Shape-based method result

plied to UVI images for auroral detection, we have found that direct application of these methods to FUV imagery produces poor results. These existing methods and the auroral oval detection results they produce for UVI imagery are described in Section 2. One reason that the existing methods for UVI imagery fail to produce accurate results for FUV imagery is that the dayglows in FUV images are much brighter than those observed in UVI images. This problem is due to the fact that the FUV sensor has a much larger field of view (15°) than the UVI sensor (8°), causing more and brighter dayglow to be imaged.

This paper is organized as follows. In Section 2, related work in auroral oval detection is presented. In Section 3, the new method is introduced. In Section 4, results of applying the new method to a set of FUV images are shown. The paper is concluded in Section 5.

2. Related Work

In this section, related works are described. We focus on the four methods that have been applied to auroral oval detection in UVI imagery. UVI is a sensor aboard the long-running NASA Polar Satellite that has acquired over 9 million images. The methods are the pulse-coupled neural network (PCNN)-based [3], histogram-based K-means (HKM) [4], adaptive minimum error thresholding (AMET) [6], and shape-based [1] methods. Although developed for UVI imagery, later in this section we exhibit application of the methods to FUV imagery. To our knowledge, these exhibits are the first application of those methods to FUV imagery.

The PCNN-based method described by Germany et al. [3] was the first method applied to aurora detection in UVI imagery. The method associates a pulse-coupled neuron (a *segmentation neuron* [8]) with each pixel in the image. Every segmentation neuron has an internal activity that is determined by combining the feeding input, which is the intensity of its associated pixel, and the linking input from neurons associated with nearby pixels. A neuron will "fire" if its internal activity is above a threshold value. The neurons associated with pixels whose intensities are above a preset threshold fire first. The output impulses of the neurons that fire first become the linking inputs to the nearby neurons. When no more neurons fire, those pixels whose associated neurons have fired are viewed as auroral oval pixels. Fig. 2(a) shows the result of applying the method to the Fig. 1(a) image.

The HKM method of Hung and Germany [4] detects the auroral oval in UVI images using a K-means approach. It first divides the image pixels into different clusters. Then, it finds the clusters with the highest intensity means and takes them as the auroral regions. Histogram information is exploited when computing the cluster means and when clustering the pixels. Fig. 2(b) shows the method's result for the Fig. 1(a) image. Since UVI data is normalized to [0..255] and FUV is floating point data, applying the PCNN-based and HKM methods' codes directly requires normalizing the intensity range of the FUV image to [0..255].

The AMET method of Li et al. [6] detects the auroral oval in UVI images by first dividing the image into subzones based on the Magnetic Local Time (MLT). MLT is related to magnetic longitude; all the points with the same magnetic longitude have the same MLT [9]. For example, when the magnetic longitude line is facing the sun, the MLT for all the points on this line is 12:00 [9]. AMET then applies minimum error thresholding [5] in each subzone. Finally, the threshold value applied to each pixel is the average of the thresholds of the three nearby subzones. Fig. 2(c) shows the result of applying AMET to the Fig. 1(a) image.

The shape-based method of Cao et al. [1] exploits the elliptic shape trait of the auroral oval to detect it in UVI images in a fully automated way. The method finds regions of high activity and then the edges of these regions. The set of edges is separated into two parts roughly corresponding to the inner and the outer boundary of the oval. Then, linear least-squares fitting (LLSF)-based randomized Hough transform (RHT) [10] is used to determine ellipses that well-model each boundary. The region between the two fitted ellipses is taken as the auroral oval. Fig. 2(d) shows the result of applying the method to the Fig. 1(a) image.

The Fig. 2 results are typical; the existing methods used for auroral oval detection for UVI images do not produce accurate results when applied to FUV imagery.

3. New Method Description

In this section, the new method is described. It has three major stages. These stages exploit domain knowledge (e.g., the auroral oval's inner boundary is completely inside its outer boundary). First, stars and part of the dayglow and the background are automatically removed based on knowledge of the aurora's location. Second, the outer boundary of the auroral oval is automatically found. Based on the found outer boundary, the inner boundary is then automatically found. Fig. 3 shows the flow of processing.

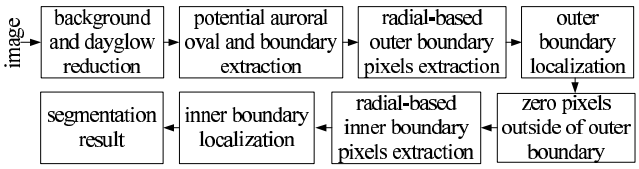

Figure 3. New method's (fully automated) processing

3.1 The Three Major Stages

Aurorae normally appear in a certain magnetic latitude (MLAT) range called the aurora zone [2]. Usually, the auroral emissions excited by precipitating protons only appear between MLAT 57.5° and 67° within the aurora zone [2]. Therefore, our method's first stage zeroes the pixels that have MLAT below 55° to 0. (We note here that the MLAT and MLT of every FUV image pixel are known.) In addition, since the dayglows should appear on the day side of the Earth, pixels that have magnetic local time between 8:00 and 15:00 are zeroed. After that, the method applies AMET to the resulting image to binarize the image into two regions. The region containing higher intensity pixels is considered to be the *foreground region* (i.e., the potential auroral oval); although it usually contains part of the dayglow, it is saved for further processing.

In the second stage, the outer boundary of the auroral oval is localized. Localization involves first extracting the boundary of the foreground region. Then, radial-based processing is used to find the outer extent of the foreground. The radial-based processing involves scanning the image along the outgoing directions from the North Pole (N) inside the foreground region to the border of the image. Point N is located by averaging the positions of the pixels whose MLAT's are very close to 90°. The boundary pixels P_i's encountered first in each radial scan of the region are ignored. The second boundary pixels encountered along the scans are taken as candidate outer boundary pixels unless they are within a small distance (e.g., 5 pixels) of a P_i pixel. We note here that since the foreground region may contain part of the dayglow, the outer boundary pixels may be from the boundary of the dayglow. To find the true auroral oval's outer boundary, the method fits an ellipse E_o to the set of candidate outer boundary pixels using LLSF-based RHT, as was described in the shape-based method for UVI of Cao et al. [1]. E_o is then taken as the true outer boundary of the auroral oval.

In the third stage, the inner boundary of the auroral oval is localized. First, the pixels outside E_o in the original image are zeroed due to the fact that the auroral oval should be completely inside E_o. Then, the method applies AMET to the resulting image to find the potential auroral oval. After that, the method extracts the inner boundary pixels using radial-based processing. This processing scans starting just inside E_o and proceeds along the directions from E_o toward N. Similar to the radial-based processing in the second stage, the boundary pixels encountered first along the scans are ignored since they are probably the outer boundary pixels. The second boundary pixels encountered along the scans are taken as inner boundary pixels unless they are too close to the outer boundary pixels (e.g., within 2 pixels). Then, an ellipse E_i is fit to the inner boundary pixels using the LLSF-based RHT. Finally, the region between E_o and E_i is taken as the auroral oval.

3.2 Processing Illustration

Fig. 4 illustrates these three stages for the FUV image shown in Fig. 4(a). Fig. 4(b) shows the result of zeroing the pixels whose MLAT is smaller than 55° and the pixels whose MLT is between 8:00 and 15:00. Fig. 4(c) shows the foreground region obtained in the first stage. Fig. 4(d) shows the extracted boundary of the foreground region in the second stage. Fig. 4(e) shows the scan directions of the radial-based processing in the second stage. Fig. 4(f) shows the extracted outer boundary pixels and the E_o. Fig. 4(g) shows the extracted inner boundary pixels and the E_i. Fig. 4(h) shows the E_o and the E_i overlaid on the original image. Fig. 4(i) shows the final result.

4 Experimental Results

This section presents some auroral oval detections from applying the new method to a set of 131 FUV images taken from five days of the year 2000. Fig. 5 shows some sample results for these images. The first row of Fig. 5 shows the original images. The second row of Fig. 5 shows the detected ellipses for the inner and the outer boundary of the auroral oval overlaid on the original image.

The 131 results accurately matched human experts in 123 (93.8%) cases. In 8 (6.2%) cases, the method's results were subpar, although there were no abject failures. Among the subpar results, 3 have inaccurate outer boundaries and 8 have inaccurate inner boundaries. One reason for the subpar results is that some images have auroral oval inner boundaries that are irregular in shape (due to substorms). Another reason is that the auroral activity in some images is very low. In those images, there is a very low contrast between the auroral oval and the background.

5 Conclusion

This paper presents, to our knowledge, the first automatic method for auroral oval detection in FUV images. The method utilizes domain knowledge of the shape and

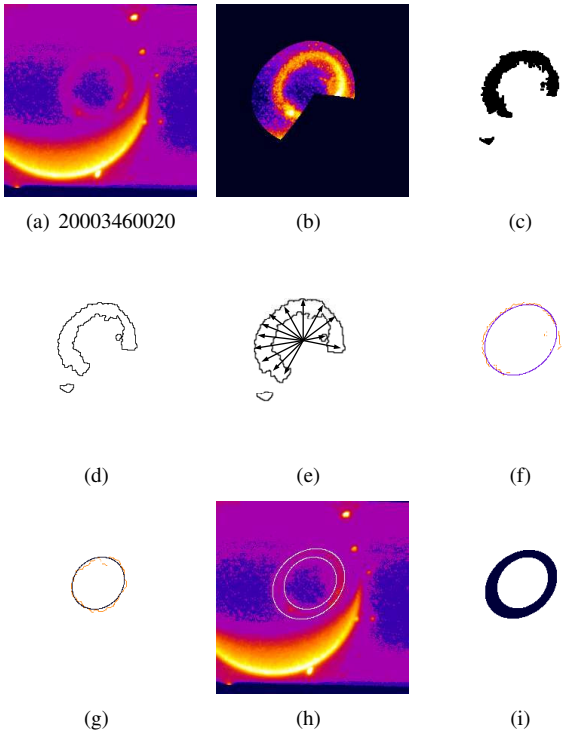

(a) 20003460020 (b) (c)

(d) (e) (f)

(g) (h) (i)

Figure 4. Illustration of processing: (a) Original image, (b) Result after background and dayglow reduction, (c) Foreground region, (d) Extracted boundary, (e) First radial-based scan directions, (f) Detected outer ellipse overlaid on the outer boundary pixels, (g) Detected inner ellipse overlaid on the inner boundary pixels, (h) Detected ellipses overlaid on the image, (i) Detection result

location of the auroral ovals to guide the detection. Experimental results show that the method is highly accurate despite the extreme low level of contrast and strong dayglows present in the images. The method might be applicable for future efforts to allow retrieval of imagery from a database of FUV images.

Acknowledgment

This work was partially funded by the NASA Science Mission Directorate under grant NNG06E60G.

References

[1] C. Cao, T. Newman, G. Germany: "Shape-Based Aurora Oval Segmentation from UVI Images," *Eos Tran. AGU*, 86(52), Abs. SM51B-1285, 2005.

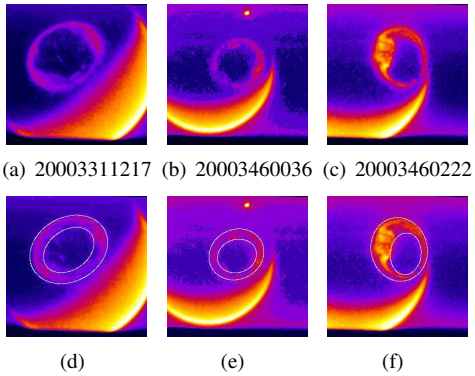

(a) 20003311217 (b) 20003460036 (c) 20003460222

(d) (e) (f)

Figure 5. Auroral oval detection results: original images (first row) and detections (second row)

[2] M. Galand, D. Lummerzheim, A. Stephan, B. Bush, S. Chakrabarti: "Electron and Proton Aurora Observed Spectroscopically in the Far Ultraviolet," *J. Geophysical Res.*, **107**(A7), pp. SIA 14-1 to 14-14, 2002.

[3] G. Germany, G. Parks, H. Ranganath, R. Elsen, P. Richards, W. Swift, J. Spann, M. Brittnacher: "Analysis of Auroral Morphology: Substorm Precursor and Onset on January 10, 1997," *Geophysical Res. Letters*, **25**, pp. 3042-3046, 1998.

[4] C. Hung, G. Germany: "K-means and Iterative Selection Algorithms in Image Segmentation," *Proc., IEEE Southeast Conf.*, Jamaica, West Indies, 2003.

[5] J. Kittler, J. Illingworth: "Minimum Error Thresholding," *Pattern Recognition*, **19**, pp. 41-47, 1986.

[6] X. Li, R. Ramachandran, M. He, S. Movva, J. Rushing, S. Graves, W. Lyatsky, A. Tan, G. Germany: "Comparing Different Thresholding Algorithms for Segmenting Auroras," *Proc., Int'l Conf. on Info. Tech.: Coding and Comp.*, pp. 594-601, Las Vegas, 2004.

[7] X. Li, R. Ramachandran, S. Movva, S. Graves, G. Germany, W. Lyatsky, A. Tan: "Dayglow Removal from FUV Auroral Images," *Proc., IEEE Int'l Geosci. and Remote Sensing Symp.*, vol. 6, pp. 3774-3777, 2004.

[8] H. Ranganath, G. Kuntimad: "Image Segmentation using Pulse Coupled Neural Networks," *Proc., IEEE Int'l Conf. Neural Nets.*, vol. 2, pp. 1285-1290, 1994.

[9] D. Stern, M. Peredo: "Get a Straight Answer," http://www-spof.gsfc.nasa.gov/Education/FAQs1.html, Accessed, July 2006.

[10] L. Xu, E. Oja, P. Kultanen: "A New Curve Detection Method: Randomized Hough Transform (RHT)," *Pattern Recog. Letters*, **11**(5), pp. 331-338, 1990.